Giant tunneling magnetoresistance in $Co_2MnSi/Al-O/Co_2MnSi$ magnetic tunnel junctions

Y. Sakuraba,[a] M. Hattori, M. Oogane, Y. Ando, H. Kato, A. Sakuma, and T. Miyazaki
Department of Applied Physics, Graduate School of Engineering, Tohoku University, Aoba-yama 6-6-05, Aramaki, Aoba-ku, Sendai 980-8579, Japan

H. Kubota
Nanoelectronics Research Institute, National Institute of Advanced Industrial Science and Technology (AIST), 1-1-1 Umezono, Tsukuba 305-8568, Japan

(Received 18 January 2006; accepted 22 March 2006; published online 10 May 2006)

Magnetic tunnel junctions (MTJs) with a stacking structure of $Co_2MnSi/Al-O/Co_2MnSi$ were fabricated using magnetron sputtering system. Fabricated MTJ exhibited an extremely large tunneling magnetoresistance (TMR) ratio of 570% at low temperature, which is the highest TMR ratio reported to date for an amorphous Al–O tunneling barrier. The observed dependence of tunneling conductance on bias voltage clearly reveals the half-metallic energy gap of Co_2MnSi. The origins of large temperature dependence of TMR ratio were discussed on the basis of the present results. © *2006 American Institute of Physics*. [DOI: 10.1063/1.2202724]

Tunneling magnetoresistance (TMR) effect in magnetic tunnel junctions (MTJs) is determined from the spin polarization in the two ferromagnetic layers.[1] Half-metallic ferromagnets (HMFs) theoretically achieve complete spin polarization of conduction electrons, potentially generating giant TMR effect and highly efficient spin injection. However, despite extensive experimental studies, half metallicity at room temperature (RT) has yet to be observed.

Perovskite manganites, $La_{1-x}(Sr,Ca,etc.)_{1-x}MnO_3$, are the first examples of HMFs, and a TMR ratio of 1800% at low temperature (LT) has been reported for a MTJ with $La_{2/3}Sr_{1/3}MnO_3$ electrodes.[2] However, such large TMR ratios and high spin polarization cannot be expected at RT for these manganites due to the low Curie temperature (T_C) of these materials (ca. 300 K). Some groups of full-Heusler alloys, such as Co_2MnSi and Co_2MnGe, are also potential HMFs, and due to their high T_C are at present the most promising materials for realizing complete spin polarization at RT.[3,4] The full-Heusler alloys represent a class of ternary intermetallic compounds with the general formula X_2YZ and structural class $L2_1$. These materials also assume $B2$ and $A2$ structures depending on the site-disordered state, in which (Y,Z) and (X,Y,Z) are randomly substituted. The half-metallic band structure in the full-Heusler alloys is predicted to be sensitive to the site-disordered state,[5,6] suggesting that a high degree of site order is necessary to realize HMF behavior in practice. Among the full-Heusler alloys, Co_2MnSi (CMS) is the most prospective HMF material because it has a high T_C (985 K) and forms the $L2_1$-ordered structure more readily than the other full-Heusler compounds.[7] Our group recently fabricated a MTJ consisting of a highly ordered Co_2MnSi epitaxial bottom electrode, Al–O tunnel barrier, and $Co_{75}Fe_{25}$ top electrode, and the device was confirmed to have a TMR ratio of 70% at RT and 159% at LT.[8] The estimated spin polarization of 0.89 at 2 K implies that the Co_2MnSi electrode has half-metallic character. However, there have been no direct observations of the half-metallic energy gap with respect to an applied bias voltage, and no clear explanation has been derived for the large temperature dependence of the TMR ratio.

In this study, MTJs with Co_2MnSi as both the upper and lower electrodes were constructed and characterized. The MTJ with a stacking structure of MgO(100) substrate/ epitaxial Cr (40)/epitaxial Co_2MnSi (30)/Al–O (1.3)/Co_2MnSi (10)/$Ir_{22}Mn_{78}$ (10)/Ta (5) (values in parentheses denote layer thickness in nanometers) was deposited using inductively coupled plasma (ICP)-assisted magnetron sputtering. A composition-adjusted Co–Mn–Si alloy sputtering target (Co, 43.7%; Mn, 27.95%; and Si, 28.35%) was used to produce a stoichiometric film composition. The (100)-oriented epitaxial Co_2MnSi bottom electrode was grown on a Cr-buffered MgO (100) substrate at ambient temperature.[9] The film was subsequently annealed at 450 °C to reduce site disorder. The upper Co_2MnSi electrode was deposited at ambient temperature followed by annealing at 400 °C prior to depositing the $Ir_{22}Mn_{78}$ antiferromagnetic pinning layer. This fabrication process suppresses the diffusion of Mn atoms in $Ir_{22}Mn_{78}$ toward the Al–O barrier during annealing, which generally degrades the interface and reduces the TMR ratio.[10] The Al–O tunnel barrier was formed by plasma oxidation of a predeposited 1.3 nm thick Al layer for 50 s. Magnetoresistance (MR) measurements were performed using a standard dc four-probe method, and the dependence of the tunneling conductance ($dI/dV-V$) on bias voltage was measured at 6 K using an ac lock-in amplifier technique.

Cross-sectional high-resolution transmission electron microscopy (HRTEM) images of the $Co_2MnSi/Al-O/Co_2MnSi$ MTJ are shown in Fig. 1. The MTJ has an excellent morphology with an smooth and flat interface as shown in Fig. 1(a). The Cr buffer layer and lower Co_2MnSi electrode display (001)-oriented epitaxial growth, as reported in previous work.[8,9] Both the lower and upper interfaces between the Al–O amorphous barrier and the Co_2MnSi electrode are very flat and sharp. Interestingly, a clear lattice image was obtained even in the upper Co_2MnSi layer [Figs. 1(b) and 1(c)], despite the nonepitaxial condition of growth on the Al–O amorphous barrier. The Fourier transform for images of several local regions of the upper Co_2MnSi layer reveals highly (001)-textured growth with

[a]Electronic mail: sakuraba@mlab.apph.tohoku.ac.jp

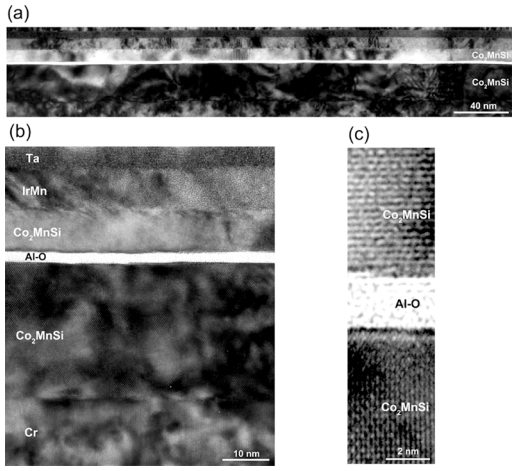

FIG. 1. (Color online) TEM images of a MTJ with $Co_2MnSi/Al-O/Co_2MnSi$ structure. The horizontal and vertical directions correspond to the bottom Co_2MnSi [110] (MgO substrate [100]) axis and Co_2MnSi [001] (MgO substrate [001]) axes, respectively. (a) Low-magnification image showing smooth structure of the MTJ in the long horizontal region. [(b) and (c)] High-magnification image and lattice image of upper and lower Co_2MnSi layers.

random in-plane orientations. These results suggest that the upper crystalline Co_2MnSi is well formed, attributable to the flatness of the lower structure and the low surface energy of the amorphous Al–O layer. Although the degree of site order could not be estimated for the upper Co_2MnSi layer due to experimental difficulties, the postannealing temperature of 400 °C is considered sufficiently high to obtain a highly ordered state.

Figure 2 shows the temperature dependence of the TMR ratio for the $Co_2MnSi/Al-O/Co_2MnSi$ MTJ (MTJ-CMS). The TMR curves at the corresponding temperature are also shown (inset), as are previous results for a $Co_2MnSi/Al-O/Co_{75}Fe_{25}$ MTJ (MTJ-CF) and a conventional $Co_{75}Fe_{25}/Al-O/Co_{75}F_{25}$ MTJ. The applied bias voltage in all measurements was ca. 1 mV. The TMR ratio of 67% observed at 300 K for the MTJ-CMS is similar to that for the MTJ-CF, yet increases dramatically with decreasing temperature to 570% at 2 K. If the spin polarization of the lower Co_2MnSi electrode is assumed to be 0.89, as suggested

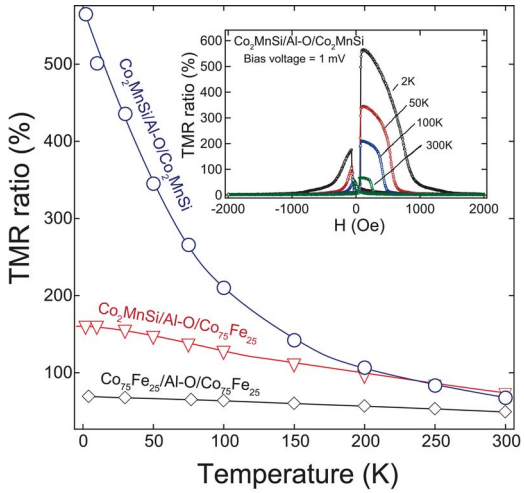

FIG. 2. (Color online) Temperature dependence of TMR ratio for the $Co_2MnSi/Al-O/Co_2MnSi$ MTJ. Data for the $Co_2MnSi/Al-O/Co_{75}Fe_{25}$ and $Co_{75}Fe_{25}/Al-O/Co_{75}Fe_{25}$ MTJs are shown for comparison. TMR curves at the corresponding temperature are shown in the inset. All measurements were conducted under an applied bias voltage of +1 mV.

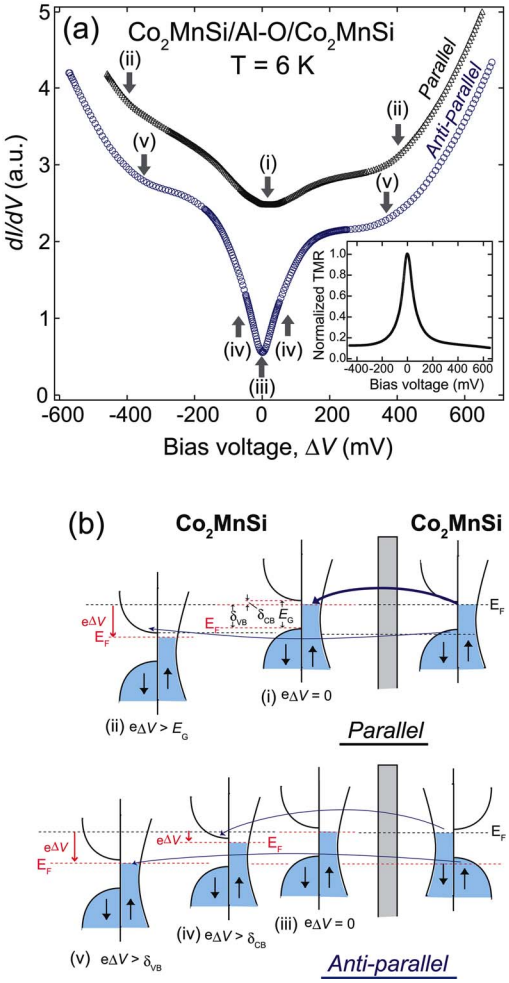

FIG. 3. (Color online) Dependence of tunnel conductance (dI/dV-V) on bias voltage for a MTJ with $Co_2MnSi/Al-O/Co_2MnSi$ structure. (a) dI/dV-V curves for parallel (triangle) and antiparallel (circle) configurations at 6 K. (Inset) Dependence of normalized TMR ratio on bias voltage. (b) Schematic of electron tunneling process at finite bias voltage in the $Co_2MnSi/Al-O/Co_2MnSi$ system for parallel and antiparallel configurations.

by previous results,[8] the spin polarization of the upper Co_2MnSi is estimated by Julliere's formula to be 0.83. This TMR ratio at LT is the largest reported for a MTJ with an Al–O barrier, and is comparable to that of a MTJ with a MgO barrier.[11]

The dependence of tunneling conductance (dI/dV-V) on the bias voltage is shown in Fig. 3 for both the parallel and antiparallel configurations. A positive bias is defined here as the case in which electron tunneling occurs from the lower to upper Co_2MnSi electrode. In the simple MTJ model,[1] the tunneling conductance is proportional to $D^L{}_M D^R{}_M + D^L{}_m D^R{}_m$ in the parallel configuration and $D^L{}_M D^R{}_m + D^L{}_m D^R{}_M$ in the antiparallel configuration. Here $D^{L(R)}{}_{M(m)}$ represents the density of states (DOS) at the Fermi energy for the majority (minority) spins of left (right) electrode. Therefore, information regarding the DOS around the Fermi energy can be determined directly from the shape of the dI/dV-V curve.[12] In the low-bias region [$10\ \text{mV} < |\Delta V| < 150\ \text{mV}$, (iv) in Fig. 3(a)], dI/dV increases sharply with increasing bias for the antiparallel configuration. This behavior is coincident with the dramatic decrease in the TMR ratio [Fig. 3(a), inset]. The voltage corresponding to half the TMR ratio at zero bias ($V_{\pm 1/2}$) is estimated to be ±60 mV, which is approximately

one-tenth of that for a conventional MTJ with 3*d* ferromagnetic metal or alloy electrode.[13] The slope of the *dI*/*dV*-*V* curve becomes shallow in the intermediate bias region ($200\ \mathrm{mV} < |\Delta V| < 350\ \mathrm{mV}$), but increases at higher bias [$350\ \mathrm{mV} < |\Delta V| < 450\ \mathrm{mV}$, (ii) and (v) in Fig. 3(a)]. To understand the relationship between the observed bias voltage dependence of *dI*/*dV* and the half-metallic band structure of Co_2MnSi, schematics of the electron tunneling process at finite bias voltages are shown in Fig. 3(b) for the parallel and antiparallel configurations. For simplicity, the ideal half-metallic DOS is assumed for both Co_2MnSi layers in Fig. 3(b). The energy separation between the Fermi level and the bottom (top) of the conduction (valence) band in the minority-spin band is represented by δ_{CB} (δ_{VB}). In the parallel configuration, the tunnel conductance is dominated by the majority-majority spin channel at $\Delta V=0$ [see (i) in Figs. 3(a) and 3(b)]. However, a new conducting channel for minority-minority spin opens when the applied voltage ΔV becomes equal to the half-metallic gap energy E_G of Co_2MnSi. From the theoretical E_G value of 400–600 meV,[3,4] the observed structure near 400 mV [(ii) in Figs. 3(a) and 3(b)] is considered to reflect the opening of the minority-minority conducting channel. In the antiparallel configuration, the tunneling conductance is very small at $\Delta V=0$ [(iii) in Figs. 3(a) and 3(b)]. However, the tunnel current starts to flow through the minority-majority spin channels when an applied bias voltage ΔV exceeds δ_{CB}/e and δ_{VB}/e. In general, the increase in *dI*/*dV* and the drop of the TMR ratio at low bias can be explained by the zero-bias conductance anomaly caused by spin-wave excitations at the ferromagnetic (FM)/barrier interface.[14–16] However, the changing in *dI*/*dV* and TMR ratio observed in the present work is too large to be explained by spin-wave excitation at the interface alone. The shape of the *dI*/*dV*-*V* curve is therefore concluded to be derived from the band structure of Co_2MnSi and creation of minority-majority spin conducting channels in the low- and high-bias regions [(iv) and (v) in Figs. 3(a) and 3(b)]. These results suggest that E_F is located immediately below the bottom edge of the conduction band in the energy gap of Co_2MnSi. The corresponding estimated values of δ_{CB} and δ_{VB}, 10–20 and 350–400 meV, are in good agreement with the predicted band structure calculated by Ishida *et al.*[3] This therefore appears to be the first direct observation of the minority energy gap and edges for half-metallic Heusler alloys.

The strong temperature dependence of the TMR ratio observed in the MTJ-CMS is an important problem to be solved to realize RT applications. As Co_2MnSi has a high Curie temperature (985 K), it is unlikely that the temperature dependence of bulk magnetization in Co_2MnSi contributes significantly to the large decrease in the TMR ratio at RT. Such strong temperature dependences of the TMR ratio are generally attributed to spin-flip tunneling caused by magnetic impurities at the FM/barrier interface or pinholes in the barrier layer.[17] The creation of magnetic impurities is a critical problem in MTJs with Co_2MnSi electrodes, as Mn and Si have a greater affinity for oxygen compared to the conventional 3*d* transition metals. Therefore, it may be possible to suppress the temperature dependence of the TMR ratio by improving the quality of the Co_2MnSi/Al–O interface, whether by changing the oxidation process of the Al–O barrier or inserting a thin oxygen-blocking layer at the interface. It should also be noted that the location of E_F in the half-metallic energy gap is an important factor in the temperature dependence of the TMR ratio. For the MTJ characterized in this study, the energy separation between E_F and the bottom of the conduction band (δ_{CB}) is small, only 10–20 meV, giving rise to a strong dependence of the TMR ratio on the bias voltage. The large decrease in the TMR ratio with increasing temperature can also be attributed to this small value of δ_{CB}, since the thermal fluctuation energy near RT is estimated to be 30–40 meV. Therefore, if the position of E_F can be shifted toward the center of the half-metallic gap without changing the band structure significantly, both the temperature dependence and bias voltage dependence of the TMR ratio may be improved. The realization of a giant TMR effect at RT through improvement of the temperature dependence of the TMR ratio in Co_2MnSi-based MTJs thus remains a challenge with respect to both practical application and research on the fundamental physics of spintronics.

The authors give special thanks to Dr. S. Yuasa of the Japanese National Institute of Advanced Industrial Science and Technology (AIST) for helpful discussion and advice. This study was supported by the IT Program of the Research Revolution 2002 (RR2002) under the title "Development of Universal Low-Power Spin Memory," by a Grant-in-Aid for Scientific Research from the Ministry of Education, Culture, Sports, Science and Technology of Japan, by the Core Research for Evolutional Science and Technology (CREST) program of the Japan Science and Technology (JST) Corporation, by the New Energy and Industrial Technology Development Organization (NEDO) grant program, and by a Japan Society for the Promotion of Science (JSPS) Research Fellowship for Young Scientists.

[1] M. Julliere, Phys. Lett. **54A**, 225 (1975).
[2] M. Bowen, M. Bibes, A. Barthélémy, J.-P. Contour, A. Anane, Y. Lemaître, and A. Fert, Appl. Phys. Lett. **82**, 233 (2003).
[3] S. Ishida, S. Fujii, S. Kashiwagi, and S. Asano, J. Phys. Soc. Jpn. **64**, 2152 (1995).
[4] I. Galanakis, P. H. Dederichs, and N. Papanikolaou, Phys. Rev. B **66**, 174429 (2002).
[5] Y. Miura, K. Nagao, and M. Shirai, Phys. Rev. B **69**, 144413 (2004).
[6] S. Picozzi, A. Continenza, and A. J. Freeman, Phys. Rev. B **69**, 094423 (2004).
[7] P. J. Webster, *Numerical Data and Functional Relationships in Science and Technology*, Landolt-Börnstein New Series III/19c (Springer, Berlin, 1988).
[8] Y. Sakuraba, J. Nakata, M. Oogane, H. Kubota, Y. Ando, A. Sakuma, and T. Miyazaki, Jpn. J. Appl. Phys., Part 2 **44**, L1100 (2005).
[9] Y. Sakuraba, J. Nakata, M. Oogane, H. Kubota, Y. Ando, A. Sakuma, and T. Miyazaki, Jpn. J. Appl. Phys., Part 1 **44**, 6535 (2005).
[10] S. Cardoso, P. P. Freitas, C. de Jesus, P. Wei, and J. C. Soares, Appl. Phys. Lett. **76**, 610 (2000).
[11] S. Ikeda, J. Hayakawa, Y. M. Lee, R. Sasaki, T. Meguro, F. Matsukura, and H. Ohno, Jpn. J. Appl. Phys., Part 2 **44**, L1442 (2005).
[12] J. M. De Teresa, A. Barthélémy, A. Fert, J. P. Contour, R. Lyonnet, F. Montaigne, P. Seneor, and A. Vaurés, Phys. Rev. Lett. **82**, 4288 (1999).
[13] S.-J. Ahn, T. Kato, H. Kubota, Y. Ando, and T. Miyazaki, Appl. Phys. Lett. **86**, 102506 (2005).
[14] J. S. Moodera, J. Nowak, and J. M. Veerdonk, Phys. Rev. Lett. **80**, 2941 (1998).
[15] Y. Ando, J. Murai, H. Kubota, and T. Miyazaki, J. Appl. Phys. **87**, 5209 (2000).
[16] S. Zhang, P. M. Levy, A. Markey, and S. S. P. Parkin, Phys. Rev. Lett. **79**, 3744 (1997).
[17] C. H. Shang, J. Nowak, R. Jansen, and J. S. Moodera, Phys. Rev. B **58**, R2917 (1998).
[18] Schmal J. Schmalhorst, S. Kämmerer, M. Sacher, G. Reiss, and A. Hütten, Phys. Rev. B **70**, 024426 (2004).